Inversion of Ferrimagnetic Magnetization by Ferroelectric Switching via a Novel Magnetoelectric Coupling

Yakui Weng,[1] Lingfang Lin,[1] Elbio Dagotto,[2,3] and Shuai Dong[1,*]
[1]Department of Physics, Southeast University, Nanjing 211189, China
[2]Department of Physics and Astronomy, University of Tennessee, Knoxville, Tennessee 37996, USA
[3]Materials Science and Technology Division, Oak Ridge National Laboratory, Oak Ridge, Tennessee 37831, USA
(Received 31 January 2016; published 12 July 2016)

Although several multiferroic materials or heterostructures have been extensively studied, finding strong magnetoelectric couplings for the electric field control of the magnetization remains challenging. Here, a novel interfacial magnetoelectric coupling based on three components (ferroelectric dipole, magnetic moment, and antiferromagnetic order) is analytically formulated. As an extension of carrier-mediated magnetoelectricity, the new coupling is shown to induce an electric-magnetic hysteresis loop. Realizations employing $BiFeO_3$ bilayers grown along the [111] axis are proposed. Without involving magnetic phase transitions, the magnetization orientation can be switched by the carrier modulation driven by the field effect, as confirmed using first-principles calculations.

DOI: 10.1103/PhysRevLett.117.037601

Magnetoelectric (ME) effects and multiferroic materials are very important both for basic science and for practical applications [1–3]. However, to realize multiferroics into concrete devices, there are several crucial physical issues still to be addressed. Not only must the ferroelectric properties, e.g., the ferroic phase transition temperatures (T_C's), magnetization ($\mathbf{M}$), and polarization ($\mathbf{P}$), be increased [1,4], but also the coupling strength between spin moments and charge dipoles should be intrinsically stronger. Although a few exceptional multiferroic materials, such as $BiFeO_3$ and its heterostructures, show promising properties [5–8], several improvements are still required to achieve direct and effective ME functions at room temperature, especially to obtain an electric-magnetic ($\mathbf{E}$-$\mathbf{M}$) hysteresis loop.

Phenomenologically, any magnetoelectric energy term can be expressed as a function of the ferroic moments $\mathbf{P}$ and $\mathbf{M}$, satisfying the energy symmetry requirement that they transform as a scalar [3]. For example, the most canonical one, $\mathbf{P}^2\mathbf{M}^2$, represents pure strain-mediated magnetoelectricity that often occurs in composites consisting of simple piezoelectric and magnetostric components. One of the most important recent achievements in multiferroics is the discovery of several other ME mechanisms beyond this simple $\mathbf{P}^2\mathbf{M}^2$. For example, a complex interaction term $\mathbf{P}\cdot[\mathbf{M}(\nabla\cdot\mathbf{M})-(\mathbf{M}\cdot\nabla)\mathbf{M}]$ was proposed [9], which is associated with the Dzyaloshinskii-Moriya interaction (or spin current) mediated ME coupling in spiral magnets [10,11].

In heterostructures, there are many other possibilities. For example, the field-effect ME coupling can be carrier mediated in heterostructures involving ferroelectrics (or dielectrics) and ferromagnets [8,12–15], and it can be expressed as $(\nabla\cdot\mathbf{P})\mathbf{M}^2$ [or $(\nabla\cdot\mathbf{P})|\mathbf{M}|$]. Microscopically, the magnetic response to electric fields is achieved by accumulating or depleting carriers (electrons or holes) near the interface via the field effect [8,14]. In this case, the sign of $\mathbf{M}$ cannot be switched, but its amplitude ($|\mathbf{M}|$) can be tuned because it is proportional to the carrier density. For correlated electronic systems, magnetic phase transitions can be obtained upon carrier modulation, which may amplify this carrier-mediated ME response [16–24]. Despite the considerable modulation of $|\mathbf{M}|$, the sign of $\mathbf{M}$ is still not switchable upon electric switching. Furthermore, magnetic phase transitions are not easy to control in real experiments, because the system must be fine-tuned to be located near phase boundaries. Realizing sensitive ME responses based on phase transitions of robust magnetic states remains a challenge.

New ME coupling: $(\nabla\cdot\mathbf{P})(\mathbf{M}\cdot\mathbf{L})$.—In this Letter, a new mechanism for ME coupling will be proposed based on the carrier-mediated field effect. This novel coupling does not depend on magnetic phase transitions, and it can lead to a 180° switching of $\mathbf{M}$. The key observation is to replace $\mathbf{M}^2$ in the aforementioned formula by $\mathbf{M}\cdot\mathbf{L}$, where $\mathbf{L}$ is the AFM order parameter. In the presence of robust AFM order (i.e., robust $\mathbf{L}$), the direction of $\mathbf{M}$ can be switched accompanying the switching of $\mathbf{P}$.

How do we realize this new ME coupling in real materials? In general, the field effect, in the form of $\nabla\cdot\mathbf{P}$, is layer dependent. Thus, antiferromagnetism realized in layered form, such as in the *A*-type AFM order, is preferred to better couple with the field effect [18,24]. However, this type of AFM order is rare in real materials. Although some manganites (e.g., $LaMnO_3$ and $Nd_{0.5}Sr_{0.5}MnO_3$) do display *A*-type AFM order [25,26], the state is fragile and is not realized in thin films [27–29].

By contrast, the most common AFM state in pseudocubic perovskites is the *G*-type rocksalt-type order [shown

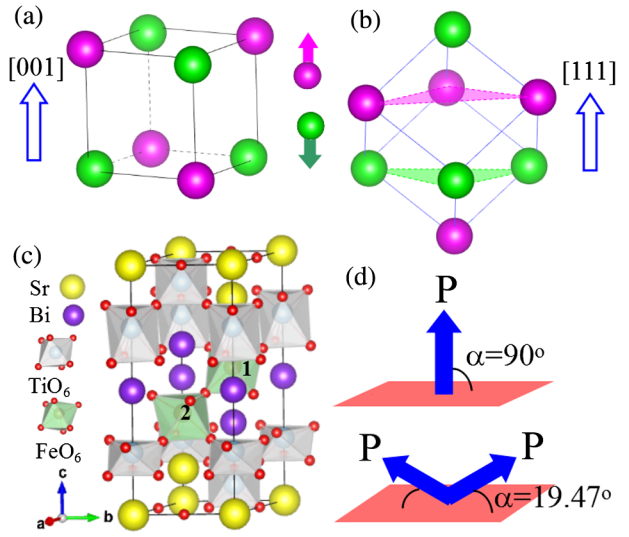

FIG. 1. (a),(b) Sketches of G-type AFM order (as in $BiFeO_3$) viewed from different orientations. The spins are distinguished by colors. (c) Sketch of a superlattice stacking along the pseudocubic [111] direction. The two Fe's are labeled as 1 and 2. (d) The possible orientations of $\mathbf{P}$, with α being the angle between $\mathbf{P}$ and the (111) plane.

in Fig. 1(a)]. However, this G-type AFM order is actually layered along the pseudocubic [111] direction, as sketched in Fig. 1(b). From this observation, we propose the $(BiFeO_3)_m/(SrTiO_3)_n$ heterostructures grown along the [111] axis [30] to realize the new $(\nabla\cdot\mathbf{P})(\mathbf{M}\cdot\mathbf{L})$ ME coupling proposed here. There are several physical considerations to discuss.

First, $BiFeO_3$ is the most studied room-temperature multiferroic perovskite with prominent ferroelectricity (a large $\mathbf{P}$ up to ~90–100 $\mu C/cm^2$ along the pseudocubic [111] axes below a high $T_C \sim 1103$ K) [31,32], which is an advantage for realizations in field effects. The robust G-type AFM state of $BiFeO_3$ ($T_N \sim 643$ K) [31] makes $\mathbf{L}$ stable during the magnetoelectric switching.

Second, $SrTiO_3$ is the most used substrate, with various terminations and orientations available [29,33]. There is plenty of experience to fabricate $BiFeO_3$-$SrTiO_3$ heterostructures layer by layer along both the [001] and [111] orientations [5–7,31,34,35]. Moreover, the different valences between Sr^{2+} and Bi^{3+} can effectively modulate the interfacial carrier density, as in $LaAlO_3$-$SrTiO_3$ heterostructures [36]. Moreover, the electron transfer between $BiFeO_3$ and $SrTiO_3$ should be negligible due to the stability of the Fe^{3+} and Ti^{4+} ions, in contrast to the $YFeO_3/YTiO_3$ (or $LaFeO_3/LaTiO_3$) heterostructures where charge transfer occurs between Fe^{3+} and Ti^{3+} [37,38]. In this sense, the $BiFeO_3$ layers are nearly perfectly isolated by $SrTiO_3$, as required.

Last but not least, because $SrTiO_3$ has a high dielectric constant [39], an applied voltage to the $BiFeO_3$-$SrTiO_3$ superlattice will mainly affect the $BiFeO_3$ layers, making the electric switching of its $\mathbf{P}$ possible. In fact, a recent experiment has observed switchable ferroelectricity of $BiFeO_3$ bilayers sandwiched by $SrTiO_3$ layers [34].

Results and discussion.—Standard density functional theory (DFT) calculations were performed to verify the design proposed above [40]. First, a superlattice constructed from a $BiFeO_3$ bilayer and $SrTiO_3$ four-layer is studied, stacked along the pseudocubic [111] axis, as shown in Fig. 1(c). Here three layers of Bi^{3+}, i.e., the double n-type interfaces, are adopted to dope one more electron to the Fe bilayer. The eight [111] directions of $\mathbf{P}$ can be classified into two groups: (i) two $\mathbf{P}$'s pointing perpendicular to the interface (up and down, or $\alpha = \pm 90°$); (ii) six $\mathbf{P}$'s with an inclination relative to the interface ($\alpha = \pm 19.47°$), as summarized in Fig. 1(d). In the following, the $\alpha = \pm 90°$ cases are the focus as the two end states of a FE-switching process.

As summarized in Table I, upon the FE switching, the local magnetic moments of the Fe ions show significant modulations, as a result of the carrier modulation of the field effect. Then, the net $\mathbf{M}$ of the bilayer is switched from $-1\mu_B$ to $+1\mu_B$, accompanying the $\mathbf{P}_{up}$ ($\alpha = +90°$) to $\mathbf{P}_{down}$ ($\alpha = -90°$) switching [57].

In this heterostructure with a Bi trilayer and a Fe bilayer, one more electron is introduced into the system confined to the quantum well made by the Fe bilayer. Because of the field effect, the occupancy weight of the two Fe layers will be different. Moreover, the intrinsic tendency toward charge ordering will lead to the ideal Fe^{2+}-Fe^{3+} configuration, which gives rise to a $\pm 1\mu_B$ net moment. Then, the FE switch will drive the switch between two magnetic-charge ordered configurations: Fe^{3+}(spin up)-Fe^{2+} (spin down) and Fe^{2+}(spin up)-Fe^{3+} (spin down) [40]. This ideal limit indeed is confirmed by our DFT calculations, as revealed in the atomic-projected density of states (pDOS). As shown in Fig. 2, for Fe_1 the spin-down channel is occupied by one electron in the $\mathbf{P}_{up}$ condition, i.e., Fe^{2+}, while the $3d$ spin-down channel of Fe_2 is empty, i.e., Fe^{3+}. This ideal Fe^{2+}-Fe^{3+} charge ordering also leads to insulating properties, compatible with the ferroelectricity of the $BiFeO_3$ bilayer.

This FE-switched charge ordering can be visualized by plotting the distribution of electrons (Fig. 3). First, the origin of ferroelectricity in the $BiFeO_3$ bilayer can be clearly seen as the bias of lone pair electrons of Bi^{3+} ions.

TABLE I. DFT results. $\mathbf{P}_{up}$ and $\mathbf{P}_{down}$ denote the $\alpha = +90°$ and $-90°$ conditions, respectively. m_1 and m_2 are the local magnetic moments for the Fe_1 and Fe_2 cations, respectively, integrated within the Wigner-Seitz spheres. M is the net bilayer magnetization. All moments in units of μ_B.

FE	m_1	m_2	M
$\mathbf{P}_{up}$	3.607	−4.170	−1
$\mathbf{P}_{down}$	4.170	−3.608	1

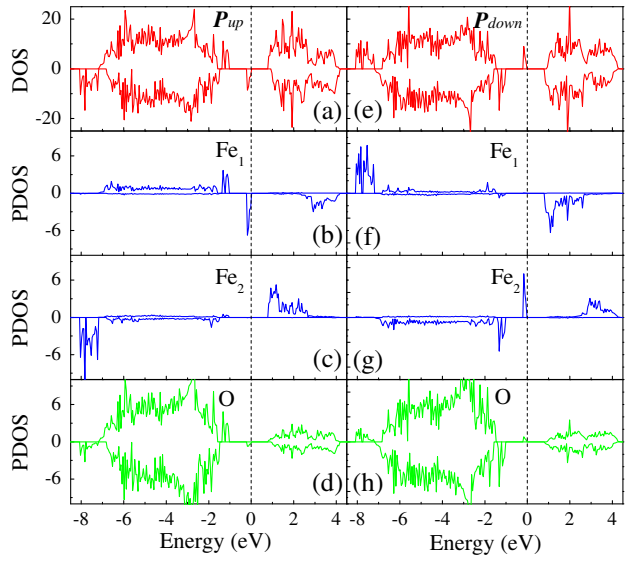

FIG. 2. Electronic structure (total DOS and pDOS) of the $BiFeO_3/SrTiO_3$ heterostructures along the [111] direction. Here, a Bi trilayer and a Fe bilayer are considered. (a)–(d) $\mathbf{P}_{up}$. (e)–(h) $\mathbf{P}_{down}$. The Fermi energy is positioned at zero.

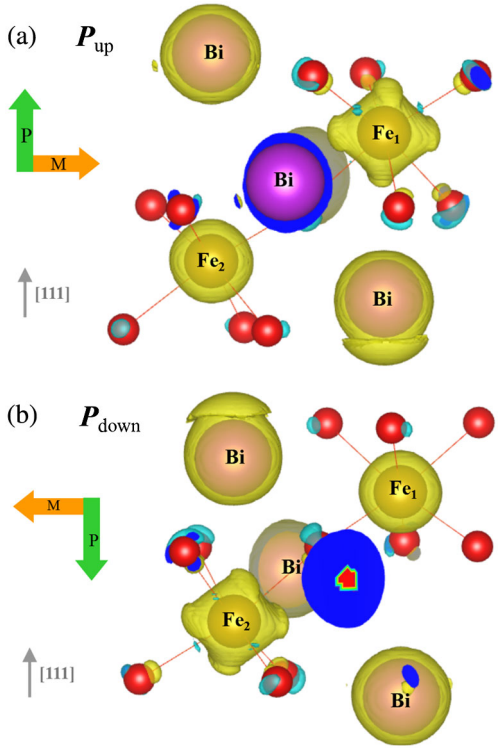

FIG. 3. Spatial distribution of the electronic density for the cases (a) $\mathbf{P}_{up}$ and (b) $\mathbf{P}_{down}$. The orientations of $\mathbf{M}$ and $\mathbf{P}$ are also indicated.

Second, the electron disproportion between Fe_1 and Fe_2 is very clear. The electron cloud surrounding the expected Fe^{3+} ion is almost spherical, while for the Fe^{2+} ion it is d_{xz} shaped (or d_{yz} shaped depending on the coordination choice) and larger in size.

Besides the two end states, the intermediate states ($\alpha = \pm 19.47°$) are also calculated, giving identical results to the corresponding $\alpha = \pm 90°$ limits (see Supplemental Material [40]). In other words, the sign of the c component of $\mathbf{P}$ uniquely determines $\mathbf{M}$, while the in-plane component does not affect this conclusion. This is reasonable considering the large spontaneous $\mathbf{P}$ of $BiFeO_3$, whose c component ($\sim 30\ \mu C/cm^2$) is already large enough for the field effect, even in the $\alpha = \pm 19.47°$ cases. The process leading to the complete electric-field switch of $\mathbf{M}$ is summarized in Fig. 4, including an $\mathbf{E}$-$\mathbf{M}$ hysteresis loop, a desired function of magnetoelectricity.

Next, it is important to estimate the working temperature of this ME function. The approximate FE transition temperature T_C can be obtained by comparing the energy difference between the paraelectric and FE phases. As summarized in Table II, the energy barrier is lowered by 29% in bilayers compared with the bulk value. However, considering the very high FE T_C (~ 1103 K) of bulk $BiFeO_3$, the expected FE T_C of the $BiFeO_3$ bilayer should remain above room temperature, a favorable property.

To estimate the magnetic transition temperature T_N, the exchange coefficient (J) is estimated by mapping the system to a classical spin model. In both bulk and bilayer systems, the nearest-neighbor J's are AFM, leading to a G-type AFM state (Table II). However, the magnitude of J is reduced in bilayers, implying that the AFM coupling between Fe^{2+} and Fe^{3+} is weaker than that between Fe^{3+} and Fe^{3+}. Considering the coordination number, the reduced dimensionality of bilayers will also suppress T_N.

Another difference between the bulk and bilayer is the magnetic anisotropy. For bulk $BiFeO_3$, with a spontaneous $\mathbf{P}$ pointing along the hexagonal z axis, the magnetic easy plane is the x–y plane. In our DFT calculation with spin-orbit coupling (SOC), the magnetocrystalline energy is about 0.084 meV/Fe, in agreement with previous DFT results [58]. In fact, such a weak magnetic anisotropy is due

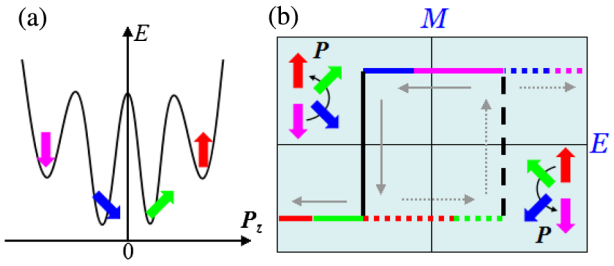

FIG. 4. (a) Sketch of energy vs the z-axis component of $\mathbf{P}$. (b) Sketch of the electric field control of magnetism. The sign of $\mathbf{M}$ is turned accompanying the switch of $\mathbf{P}$, forming an $\mathbf{E}$-$\mathbf{M}$ hysteresis loop. The maximum saturated $|\mathbf{M}|$ can reach $0.5\mu_B$/Fe. The coercivity is determined by the FE coercivity of the $BiFeO_3$ layers. Even without the $\alpha = \pm 90°$ end states, an $\mathbf{E}$-$\mathbf{M}$ hysteresis loop can also be achieved between the $\alpha = \pm 19.47°$ cases.

TABLE II. Summary of the calculated FE barrier ΔE, exchange coefficient J (with normalized spins $|\mathbf{S}| = 1$), and magnetocrystalline energy (E_K), all in units of meV/Fe. Three perpendicular spin axes [(x, y, z), z perpendicular to the bilayer] are adopted to calculate E_K, and the energy for spins along the z axis [$E_K(z)$] is taken as a reference.

	ΔE	J	$E_K(x)$	$E_K(y)$
Bulk	581	39.72	−0.084	−0.084
$\alpha = \pm 90°$	414	26.83	0.165	−0.250

to the Dzyaloshinskii-Moriya interaction, a high-order SOC effect, since the orbit moment of the high-spin $3d^5$ configuration is almost quenched. By contrast, in the $BiFeO_3/SrTiO_3$ heterostructures, a magnetocrystalline easy axis (y axis) is found due to the spin-down d_{xz} electron of Fe^{2+}, whose effective SOC is relatively large. Such a strong magnetocrystalline easy axis, rendering spins to be Ising-like, will be advantageous to increase T_N. Using the coefficients (exchange and magnetocrystalline anisotropy; see Table II) extracted from DFT calculations, a crude Monte Carlo (MC) simulation has been performed to estimate the phase transition temperatures [40]. For the two end states ($\alpha = \pm 90°$), the simulated T_N of bilayers is about ∼139 K. However, this T_N can be significantly improved by using thicker Fe layers, as shown below.

The calculations above have been done for ideal three Bi plus two Fe layers. In real superlattices, interfacial roughness may be present to some extent. It is necessary to check the stability of the above-described ME function beyond the ideal conditions. To pursue this goal, the layer numbers of both Fe and Bi are changed to verify the ME function. Of course, the layer number of Fe must be even, or the net $\mathbf{M}$ cannot be flipped by the field effect. Then, besides the smooth interfaces, several hybrid cases with rough Bi layers have also been tested by using an (in-plane) doubling cell. As summarized in Table III, it is clear that the only condition for the ME function is the nonstoichiometry between Bi and Fe, i.e., to have extra carriers no matter whether electrons or holes. In real experiments, even for those configurations with equivalent numbers of Bi and Fe layers (e.g., $2 + 2$), the proposed ME function remains valid once there is additional nonstoichiometry caused, e.g., by oxygen or Bi vacancies.

The ME function can also exist in thicker Fe layers, e.g., four Fe plus five Bi. Of course, the average $|\mathbf{M}|$ per Fe will decrease with the thickness of Fe, since the inner Fe layers will not contribute to $\mathbf{M}$ as much as the two interfacial layers. Even with this caveat, the thicker Fe cases can give rise to a moderate $|\mathbf{M}|$ and more stable AFM order (unflipped during the ME switching) as well as enhanced T_N, e.g., ∼371 K for four Fe plus five Bi from the MC simulation [40], a favorable property.

TABLE III. Validity of the proposed ME function in various conditions. All nonzero $\mathbf{M}$ (μ_B/Fe units) can be switched.

Bi layer	1	2	3	$1+2$	$2+3$	$1+3$	5
Fe layer	2	2	2	$2+2$	$2+2$	$2+2$	4
$\lvert\mathbf{M}\rvert$	0.5	0	0.5	0.25	0.25	0	0.24

Let us reinterpret our DFT results in the context of the Landau theory. As stated before, the field effect can be represented by a nonzero $\nabla \cdot \mathbf{P}$. Here, this field effect breaks the symmetry of the two end Fe layers. The bilayer AFM order parameter ($\mathbf{L}$) can be expressed as $\mathbf{M}_1 - \mathbf{M}_2$, where the subscript is the layer index. This order parameter $\mathbf{L}$ is unchanged during the FE-magnetic switch, which is determined only by the initial condition. Considering the energy term $(\nabla \cdot \mathbf{P})(\mathbf{M} \cdot \mathbf{L})$, the net magnetic moment $\mathbf{M}$ can be switched accompanying the flipping of $\mathbf{P}$, as proposed in the beginning. The only condition is that $|\mathbf{M}|$ be nonzero, corresponding to a net ferrimagnetic moment ($\mathbf{M}_1 + \mathbf{M}_2$) from the extra carriers (electrons or holes). Then, the phenomenological energy for the novel ME coupling can be described by

$$F \sim (\nabla \cdot \mathbf{P})(\mathbf{M} \cdot \mathbf{L}) = (\nabla \cdot \mathbf{P})[\mathbf{M}_1^2 - \mathbf{M}_2^2].$$

Thus, our proposed ME function can be considered as a backcoupling of two carrier-mediated ME interfaces.

Finally, note that some recent advances in ME heterostructures reported the 180° rotation of $\mathbf{M}$ by electric fields in metal-ferroelectric heterostructures [59,60]. However, the physical mechanism relates with a process-dependent dynamics of magnetic moments (a sequence of two 90° $\mathbf{M}$ rotations [61]). The primary driving force in these devices is the piezostrain-modulated magnetocrystalline anisotropy, and usually an assisting small magnetic field is needed [62]. An alternative route is to tune the long-range interaction (via the field effect) between two ferromagnetic layers separated by a nonmagnetic metal [63]. Although pursuing a similar function, our design is conceptually different from these previous efforts.

Summary.—To pursue the electric field control of magnetism, a new magnetoelectric coupling based on the field effect is here proposed, formally expressed as $(\nabla \cdot \mathbf{P})(\mathbf{M} \cdot \mathbf{L})$. This new magnetoelectric coupling can realize the intrinsic 180° flipping of magnetization accompanying the ferroelectric switching, while previously considered magnetoelectric couplings based on the field effect can only modulate the magnetization amplitude. The new proposal is here predicted to be realized in practice using a few layers of $BiFeO_3$ (111) sandwiched in $SrTiO_3$. Benefiting from the robust G-type AFM state of $BiFeO_3$ and its prominent ferroelectricity, the net magnetization of $BiFeO_3$, of the order of $0.5\mu_B$/Fe, can be unambiguously switched by 180° when flipping the ferroelectric polarization, leading to the expected $\mathbf{E}$-$\mathbf{M}$ hysteresis loop. Although only $BiFeO_3$ is studied here, our design principle based on $(\nabla \cdot \mathbf{P})(\mathbf{M} \cdot \mathbf{L})$ can be extended to other

magnetoelectric systems with polarization and antiferromagnetism and may lead to practical magnetoelectric devices.

We acknowledge discussions with Hangwen Guo, Pu Yu, Xiaofang Zhai, Jinxing Zhang, and Junling Wang. This work was mainly supported by the National Natural Science Foundation of China (Grants No. 11274060 and No. 51322206), the Fundamental Research Funds for the Central Universities, Scientific Research Foundation of Graduate School of Southeast University (Grant No. YBJJ1619), and Jiangsu Innovation Projects for Graduate Student (Grant No. KYLX15_0112). E. D. was supported by the U.S. DOE, Office of Basic Energy Sciences, Materials Sciences and Engineering Division.

*Corresponding author.
sdong@seu.edu.cn

[1] S.-W. Cheong and M. Mostovoy, Nat. Mater. **6**, 13 (2007).
[2] R. Ramesh and N. A. Spaldin, Nat. Mater. **6**, 21 (2007).
[3] S. Dong, J.-M. Liu, S.-W. Cheong, and Z. Ren, Adv. Phys. **64**, 519 (2015).
[4] S. Dong and J.-M. Liu, Mod. Phys. Lett. B **26**, 1230004 (2012).
[5] J. T. Heron, D. G. Schlom, and R. Ramesh, Applied Physics Reviews **1**, 021303 (2014).
[6] P. Yu, Y. H. Chu, and R. Ramesh, Phil. Trans. R. Soc. A **370**, 4856 (2012).
[7] C. L. Lu, W. J. Hu, Y. F. Tian, and T. Wu, Appl. Phys. Rev. **2**, 021304 (2015).
[8] X. Huang and S. Dong, Mod. Phys. Lett. B **28**, 1430010 (2014).
[9] M. Mostovoy, Phys. Rev. Lett. **96**, 067601 (2006).
[10] H. Katsura, N. Nagaosa, and A. V. Balatsky, Phys. Rev. Lett. **95**, 057205 (2005).
[11] I. A. Sergienko and E. Dagotto, Phys. Rev. B **73**, 094434 (2006).
[12] J. M. Rondinelli, M. Stengel, and N. A. Spaldin, Nat. Nanotechnol. **3**, 46 (2008).
[13] C.-G. Duan, J. P. Velev, R. F. Sabirianov, Z. Zhu, J. Chu, S. S. Jaswal, and E. Y. Tsymbal, Phys. Rev. Lett. **101**, 137201 (2008).
[14] C. A. F. Vaz, J. Phys. Condens. Matter **24**, 333201 (2012).
[15] M. Fechner, I. V. Maznichenko, S. Ostanin, A. Ernst, J. Henk, P. Bruno, and I. Mertig, Phys. Rev. B **78**, 212406 (2008).
[16] C. A. F. Vaz, J. Hoffman, Y. Segal, J. W. Reiner, R. D. Grober, Z. Zhang, C. H. Ahn, and F. J. Walker, Phys. Rev. Lett. **104**, 127202 (2010).
[17] H. J. A. Molegraaf, J. Hoffman, C. A. F. Vaz, S. Gariglio, D. van der Marel, C. H. Ahn, and J.-M. Triscone, Adv. Mater. **21**, 3470 (2009).
[18] J. D. Burton and E. Y. Tsymbal, Phys. Rev. B **80**, 174406 (2009).
[19] J. D. Burton and E. Y. Tsymbal, Phys. Rev. Lett. **106**, 157203 (2011).
[20] S. Dong, X. T. Zhang, R. Yu, J.-M. Liu, and E. Dagotto, Phys. Rev. B **84**, 155117 (2011).
[21] H. Chen and S. Ismail-Beigi, Phys. Rev. B **86**, 024433 (2012).
[22] Y. W. Yin, J. D. Burton, Y. Kim, A. Y. Borisevich, S. J. Pennycook, S. M. Yang, T. W. Noh, A. Gruverman, X. G. Li, E. Y. Tsymbal, and Q. Li, Nat. Mater. **12**, 397 (2013).
[23] L. Jiang, W. S. Choi, H. Jeen, S. Dong, Y. Kim, M.-G. Han, Y. Zhu, S. Kalinin, E. Dagotto, T. Egami, and H. N. Lee, Nano Lett. **13**, 5837 (2013).
[24] S. Dong and E. Dagotto, Phys. Rev. B **88**, 140404(R) (2013).
[25] E. O. Wollan and W. C. Koehler, Phys. Rev. **100**, 545 (1955).
[26] E. Dagotto, T. Hotta, and A. Moreo, Phys. Rep. **344**, 1 (2001).
[27] A. Bhattacharya, S. J. May, S. G. E. te Velthuis, M. Warusawithana, X. Zhai, B. Jiang, J.-M. Zuo, M. R. Fitzsimmons, S. D. Bader, and J. N. Eckstein, Phys. Rev. Lett. **100**, 257203 (2008).
[28] S. Dong, R. Yu, S. Yunoki, G. Alvarez, J.-M. Liu, and E. Dagotto, Phys. Rev. B **78**, 201102(R) (2008).
[29] M. Gibert, P. Zubko, R. Scherwitzl, J. Íñiguez, and J.-M. Triscone, Nat. Mater. **11**, 195 (2012).
[30] D. Xiao, W. Zhu, Y. Ran, N. Nagaosa, and S. Okamoto, Nat. Commun. **2**, 596 (2011).
[31] J. Wang, J. B. Neaton, H. Zheng, V. Nagarajan, S. B. Ogale, B. Liu, D. Viehland, V. Vaithyanathan, D. G. Schlom, U. V. Waghmare, N. A. Spaldin, K. M. Rabe, M. Wuttig, and R. Ramesh, Science **299**, 1719 (2003).
[32] T. Choi, S. Lee, Y. J. Choi, V. Kiryukhin, and S.-W. Cheong, Science **324**, 63 (2009).
[33] F. Sánchez, C. Ocal, and J. Fontcuberta, Chem. Soc. Rev. **43**, 2272 (2014).
[34] E. Bruyer, A. Sayede, A. Ferri, R. Desfeux, R. V. K. Mangalam, R. Ranjith, and W. Prellier, Appl. Phys. Lett. **107**, 042904 (2015).
[35] J. L. Blok, X. Wan, G. Koster, D. H. A. Blank, and G. Rijnders, Appl. Phys. Lett. **99**, 151917 (2011).
[36] N. Nakagawa, H. Y. Hwang, and D. A. Muller, Nat. Mater. **5**, 204 (2006).
[37] J. E. Kleibeuker, Z. Zhong, H. Nishikawa, J. Gabel, A. Müller, F. Pfaff, M. Sing, K. Held, R. Claessen, G. Koster, and G. Rijnders, Phys. Rev. Lett. **113**, 237402 (2014).
[38] H. M. Zhang, Y. K. Weng, X. Y. Yao, and S. Dong, Phys. Rev. B **91**, 195145 (2015).
[39] H. W. Guo, J. Noh, S. Dong, P. Rack, Z. Gai, X. S. Xu, E. Dagotto, J. Shen, and T. Ward, Nano Lett. **13**, 3749 (2013).
[40] See Supplemental Material at http://link.aps.org/supplemental/10.1103/PhysRevLett.117.037601 for more details of methods, more results, and experimental considerations, which includes Refs. [29,33–35,41–56].
[41] J. P. Perdew, A. Ruzsinszky, G. I. Csonka, O. A. Vydrov, G. E. Scuseria, L. A. Constantin, X. Zhou, and K. Burke, Phys. Rev. Lett. **100**, 136406 (2008).
[42] G. Kresse and J. Hafner, Phys. Rev. B **47**, 558 (1993).
[43] G. Kresse and J. Furthmüller, Phys. Rev. B **54**, 11169 (1996).
[44] S. L. Dudarev, G. A. Botton, S. Y. Savrasov, C. J. Humphreys, and A. P. Sutton, Phys. Rev. B **57**, 1505 (1998).

[45] F. Kubel and H. Schmid, Acta Crystallogr. Sect. B **46**, 698 (1990).
[46] J. B. Neaton, C. Ederer, U. V. Waghmare, N. A. Spaldin, and K. M. Rabe, Phys. Rev. B **71**, 014113 (2005).
[47] F. Gao, Y. Yuan, K. F. Wang, X. Y. Chen, F. Chen, J.-M. Liu, and Z. F. Ren, Appl. Phys. Lett. **89**, 102506 (2006).
[48] I. Sosnowska, W. Schäfer, W. Kockelmann, K. H. Andersen, and I. O. Troyanchuk, Appl. Phys. A **74**, s1040 (2002).
[49] J. F. Li, J. Wang, N. Wang, F. Bai, B. Ruette, A. P. Pyatakov, M. Wuttig, R. Ramesh, A. K. Zvezdin, and D. Viehland, Appl. Phys. Lett. **84**, 5261 (2004).
[50] S. Dong, R. Yu, S. Yunoki, J.-M. Liu, and E. Dagotto, Phys. Rev. B **78**, 064414 (2008).
[51] S. Dong, R. Yu, S. Yunoki, J.-M. Liu, and E. Dagotto, Phys. Rev. B **78**, 155121 (2008).
[52] P. Yu, W. Luo, D. Yi, J. X. Zhang, M. D. Rossell, C.-H. Yang, L. You, G. Singh-Bhalla, S. Y. Yang, Q. He, Q. M. Ramasse, R. Erni, L. W. Martin, Y. H. Chu, S. T. Pantelides, S. J. Pennycook, and R. Ramesh, Proc. Natl. Acad. Sci. U.S.A. **109**, 9710 (2012).
[53] Y. H. Chu, T. Zhao, M. P. Cruz, Q. Zhan, P. L. Yang, L. W. Martin, M. Huijben, C. H. Yang, F. Zavaliche, H. Zheng, and R. Ramesh, Appl. Phys. Lett. **90**, 252906 (2007).
[54] H. Béa, S. Fusil, K. Bouzehouane, M. Bibes, M. Sirena, G. Herranz, E. Jacquet, J.-P. Contour, and A. Barthélémy, Jpn. J. Appl. Phys. **45**, L187 (2006).
[55] P. Maksymovych, M. Huijben, M. Pan, S. Jesse, N. Balke, Y.-H. Chu, H. J. Chang, A. Y. Borisevich, A. P. Baddorf, G. Rijnders, D. H. A. Blank, R. Ramesh, and S. V. Kalinin, Phys. Rev. B **85**, 014119 (2012).
[56] D. D. Fong, G. B. Stephenson, S. K. Streiffer, J. A. Eastman, O. Auciello, P. H. Fuoss, and C. Thompson, Science **304**, 1650 (2004).
[57] The ME coefficient, defined as $d\mathbf{M}/d\mathbf{E}$, can be roughly estimated as $|\Delta\mathbf{M}|/E_c$ where the change of magnetization $|\Delta\mathbf{M}|$ is about 155 G (i.e., $0.5\mu_B$/Fe) and the coercive electric field E_c for $BiFeO_3$ is of the order of 10–100 kV/cm depending on material details [31,32,34]. Thus, α is estimated as 0.0155–0.00155 G cm/V, comparable to other ME heterostructures [63,64].
[58] C. Ederer and N. A. Spaldin, Phys. Rev. B **71**, 060401(R) (2005).
[59] M. Ghidini, R. Pellicelli, J. L. Prieto, X. Moya, J. Soussi, J. Briscoe, S. Dunn, and N. Mathur, Nat. Commun. **4**, 1453 (2013).
[60] S.-W. Yang, R.-C. Peng, T. Jiang, Y.-K. Liu, L. Feng, J.-J. Wang, L.-Q. Chen, X.-G. Li, and C.-W. Nan, Adv. Mater. **26**, 7091 (2014).
[61] J.-M. Hu, T. N. Yang, J. J. Wang, H. B. Huang, J. X. Zhang, L.-Q. Chen, and C.-W. Nan, Nano Lett. **15**, 616 (2015).
[62] J. J. Wang, J. M. Hu, J. Ma, J. X. Zhang, L. Q. Chen, and C. W. Nan, Sci. Rep. **4**, 7507 (2014).
[63] M. Fechner, P. Zahn, S. Ostanin, M. Bibes, and I. Mertig, Phys. Rev. Lett. **108**, 197206 (2012).
[64] C.-G. Duan, S. S. Jaswal, and E. Y. Tsymbal, Phys. Rev. Lett. **97**, 047201 (2006).